STM JOURNALS

Journal of
Polymer & Composites

ISSN: 2321-2810 (Online)
ISSN: 2321-8525 (Print)
Volume 14, Issue 1, 2026
DOI (Journal): 10.37591/JoPC

https://journals.stmjournals.com/jopc

Research JoPC

Thermal Stability and Impact Performance of Basalt–Carbon Hybrid Laminates in Polyimide–Phenolic Matrices

Sathish Rengarajan[1],*, Ashwin Roy[2], D. Vijayan[3], A. Geetha Selvarani[4], Jagadeesh Palanisamy[5], Pravinkumar K[6], Seshagiri Rao Vaddi[7], S. Baskar[8]

Abstract

The impact resistance and thermal stability of the advanced polymer composites are properties that are necessary for the components that are subjected to dynamic conditions, which show the overall reliability and service performance of the laminates applied in automotive structures, protective casings, etc. These properties prevent premature softening or breakdown during long-term exposure to heat. Impact resistance and thermal stability of composite laminates are studied based on fiber orientation and composition. Basalt and carbon fibers were reinforced in a new polyimide/phenolic resin framework processed in methane and propane derivatives of hybrid composites. Composite laminates were manufactured through compression molding, and their behavior under low-velocity impact loading was assessed at two distinct velocities – 2.89 m/s and 4.42 m/s – to determine the most effective fiber arrangement and hybrid configuration for achieving greater damage tolerance. Techniques such as thermogravimetric analysis (TGA), differential thermal analysis (DTA), differential scanning calorimetry (DSC), and Fourier transform infrared spectroscopy (FTIR) were employed to evaluate thermal degradation patterns, phase transitions, and chemical structure stability. The combined influence of the tailored resin chemistry and basalt–carbon hybrid reinforcement significantly enhanced both impact strength and thermal resistance. The increase in material toughness and energy absorption shows an increase in the glass transition temperature and initial decomposition temperature at 5% mass loss.

***Author for Correspondence**
Sathish Rengarajan
E-mail id: sathishr@stjosephs.ac.in

[1,7]Professor, Department of Mechanical Engineering, St. Joseph's College of Engineering, OMR, Chennai, Tamil Nadu, India
[2]Software Developer, Xerago, Industrial Estate, Perungudi, Chennai, Tamil Nadu, India
[3]Assistant Professor, Department of Mechanical Engineering, Sri Chandrasekharendra Saraswathi Viswa Mahavidyalaya, Enathur, Kanchipuram, Tamil Nadu, India
[4]Professor, Department of Civil Engineering, Vel Tech Rangarajan Dr. Sagunthala R& D Institute of Science and Technology, Avadi, Chennai, Tamil Nadu, India
[5]Assistant Professor, Department of Mechanical Engineering, K.S.R. College of Engineering, Tiruchengode, Tamil Nadu, India
[6]Assistant Professor, Department of Mechanical Engineering, St. Joseph's College of Engineering, OMR, Chennai, Tamil Nadu, India
[8]Assistant Professor, Department of Mechanical Engineering, Vels Institute of Science, Technology & Advanced Studies, Chennai, Tamil Nadu, India

Received Date: November 22, 2025
Accepted Date: December 01, 2025
Published Date: January 05, 2026

Citation: Sathish Rengarajan, Ashwin Roy, D. Vijayan, A. Geetha Selvarani, Jagadeesh Palanisamy, Pravinkumar K, Seshagiri Rao Vaddi, S. Baskar. Thermal Stability and Impact Performance of Basalt–Carbon Hybrid Laminates in Polyimide–Phenolic Matrices. Journal of Polymer & Composites. 2026; 14 (1): 247–260p.

Keywords: Basalt fiber, carbon fiber, energy absorption, hybrid composites, impact resistance

INTRODUCTION

FRP laminates are finding use in aerospace, automotive, marine, and defense applications because of their high specific strength, stiffness, and corrosion resistance [1]. In spite of those benefits, laminated composites that are susceptible to out-of-plane loads can also produce almost invisible impact damage [BVID] that itself can weaken the remaining compressive strength [2,3]. The common types of damage are matrix cracking, fiber-matrix debonding, delamination, and fiber fracture, which are irrelevant structures to more intensity than the energy absorbed [4]. Designing

FRP laminates is largely a challenge in terms of the impact tolerance [5]. The fiber hybridization is an efficient method in giving balance to the stiffness and toughness in FRP laminates [6]. Recent research has demonstrated that hybrid systems have synergistic actions including crack displacement, redistribution of energy, and delayed perforation to enhance impact resistance [7,8]. Basalt–carbon hybrids are the most promising of them. Carbon fibers offer high toughness, thermal stability at temperatures up to 800 °C, but is fragile, brittle, and costly, whereas basalt fiber made volcanic rock offers high toughness, modulus, and a greater temperature limit [9,10]. Experimental evidence confirms that incorporating basalt plies on the impacted side reduces delamination and perforation, while carbon plies maintain stiffness and load-bearing capacity [11,12]. This synergy enhances residual strength, impact energy absorption, and thermal endurance, making basalt–carbon hybrids attractive alternatives to traditional carbon–glass or carbon–aramid systems [13,14]. While the fiber reinforcement is critical, the polymer matrix largely dictates thermal stability, oxidative resistance, and fire performance. Conventional epoxies dominate current FRP systems, but their relatively low glass transition temperature [Tg < 200 °C] and poor flame resistance restrict high-temperature applications [15]. Phenolic resins provide excellent flame retardancy and high char yield but suffer from brittleness, whereas polyimides exhibit outstanding thermal stability [>500 °C] and oxidative resistance but require chemical tailoring to enhance toughness [16,17]. Recent advances in modified phenolic and polyimide matrices, including POSS-, DDSQ-, and phosphate-modified phenolics, as well as polyimides reinforced with nanofillers or hydrocarbon derivatives, have demonstrated significant improvements in Tg, decomposition onset temperature [T5%], and impact resistance [18,19]. Such resin systems extend the service capability of hybrid composites beyond that achievable with conventional epoxies. Extensive research has been carried out on carbon–glass and carbon–aramid hybrid composites, comparatively fewer studies have explored carbon–basalt hybrids, particularly with advanced high-temperature matrices. Most reported systems rely on epoxy, which softens above 200 °C limiting their use in aerospace and defense structures. The present work addresses this gap by employing a polyimide/phenolic resin system synthesized from methane and propane derivatives, which combines the high glass-transition temperature and oxidative stability of polyimides with the flame retardancy and char yield of phenolics. This hybrid resin not only enhances thermal endurance but also improves interlaminar bonding and impact energy absorption compared to conventional epoxy matrices. Consequently, the developed basalt–carbon fiber/polyimide–phenolic laminates offer a unique balance of stiffness, toughness, and high-temperature resistance, making them highly suitable for aerospace and defense applications where impact tolerance, thermal stability, and cost-effectiveness are simultaneously critical [20–24]. In this context, basalt–carbon fiber hybrids combined with polyimide/phenolic resin matrices offer an integrated solution: basalt fibers mitigate the brittleness of carbon while improving energy absorption; carbon fibers ensure stiffness and strength; and the tailored PI/phenolic matrix maintains structural integrity under high thermal and oxidative loads. Therefore, the present work fabricates and characterizes novel basalt–carbon/PI–phenolic hybrid laminates, evaluating their LVI performance at two velocities alongside thermogravimetric, differential scanning calorimetry, and FTIR analyses to establish structure-property correlations in specific applications.

Figure 1. [a] Compression molding machine with heating coil.

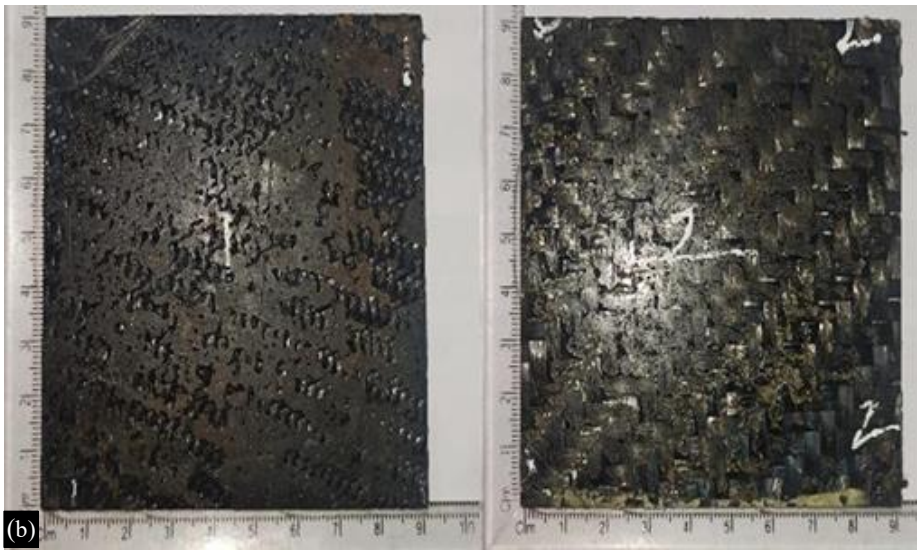

Figure 1. [b] Sample of laminates.

MATERIALS AND METHODS

Preparation of Laminates and Testing Methods

The stacking sequence was selected to make a hybrid composite laminates which was stacked 0°, ±45°, and 90° orientations by placing carbon layers on the stiffer load-bearing sides and basalt layers on the impact-resistant/thermal-stable surfaces. The optimized sequence alternates carbon and basalt so that carbon provides stiffness while basalt enhances toughness and thermal endurance using Toray T700 carbon fibers [7 μm diameter, modulus 230 GPa, tensile strength 4900 MPa] and plain-woven basalt fibers [200 g/m²] reinforced with a novel polyimide/phenolic resin system synthesized from bisphenol-A dicyanate [BDM], bis[maleimide-phenoxy] propane [BMPP], and 4,4′-diaminodiphenyl ether [DABPA]. In brief, DABPA was reacted with stoichiometric BDM and BMPP at 130–135 °C under stirring for 30 minutes and then vacuum-degassed at 120–125 °C for 90 minutes to eliminate entrapped moisture and gases. The resulting prepolymer was cast into silicone-release-coated metallic molds and subjected to a heating schedule of 165 °C for 2 h, 180 °C for 2 h, 200 °C for 2 h, and 238 °C for 4 h, followed by a 250 °C post-cure for 5 h to ensure complete crosslinking and enhanced thermal resistance [25]. Laminates [90 mm × 90 mm × 3 mm] were produced using a hand lay-up procedure combined with compression molding shown in [Figure 1[a,b]], the fibers were stacked at 0°, 90°, ±45° orientations, resin was applied and rolled for uniform impregnation, followed by consolidation under 10 bar pressure through sequential curing at 100 °C for 1 h, 150 °C for 1 h, 180 °C for 1 h, and 200 °C for 2 h to improve interface quality and reduce porosity [26]. After curing, specimens were trimmed to ASTM D7136 dimensions using abrasive waterjet cutting to avoid thermal damage at edges [27].

Thermal and structural characterization included TGA/DTG, DSC, and FTIR. TGA/DTG experiments were performed on 8 mg sample pieces heated from 30–900 °C at 10 °C/min under air flow, which enabled the determination of degradation onset and peak mass-loss rates [28]. DSC was performed under nitrogen from 30–500 °C [10 °C/min] to identify the glass transition, curing exotherms, and decomposition [29]. FTIR spectra were recorded in ATR mode across 4000–400 cm^{-1} to observe functional groups [C=O, C–N, aromatic C=C, O–H] indicative of crosslinking and fiber–matrix bonding. Low-velocity impact tests were conducted in accordance with ASTM D7136 using a drop-weight impact tester. Specimens were clamped and impacted by a 12.7 mm steel hemispherical striker at velocities of 2.89 m/s and 4.42 m/s achieved via calibrated drop heights. At the same time, the force–time, force–displacement, and energy–deformation data were recorded [30]. To study the sustainability of the composite [31] included the egg shell powder was included in jute fiber, and their effects were studied. Mechanical properties studied hybrid fiber which are utilized in E vehicles [32]. Increasing sawdust as filler material improves bending strength and modulus [33]. The addition of SiC

in ACF shows the improvement in flexural and other properties [34]. Tamarind powder is reinforced in Palmyra Palm Leaflet and Coconut Sheath Leaf and identified that there is an enhancement of bonding and better dispersion of the filler, which results in fewer voids and defects [35]. Calamus tenuis fiber is used in epoxy composites, and it shows that the damping decreases while the maximum 25%wt. percentage amount of reinforcement is included [36].

RESULTS AND DISCUSSION

Mechanical Characterization

Impact Testing

The impact test at a low velocity of 2.89 m/s. The force–deformation curves (fig. 2) indicate progressive load increase with limited oscillations, indicating stable energy absorption dominated by elastic–plastic deformation and matrix microcracking. The hybrid laminate dissipates energy through multiple mechanisms: crack initiation at resin-rich regions, fiber–matrix debonding, and limited fiber breakage. Basalt fibers, owing to their higher strain-to-failure compared to carbon, act as energy absorbers, delaying catastrophic fracture and contributing to higher deformation before failure. This balance between carbon's stiffness and basalt's toughness results in higher load-bearing capacity with controlled deformation; such behavior is consistent with studies where hybridization improves impact resistance compared with pure carbon laminates [37].

At the higher velocity of 4.42 m/s, the force–deformation response in Figure 3, shows steeper load rises followed by pronounced oscillations and step-like force drops, signifying progressive damage accumulation including matrix cracking, delamination, and localized fiber breakage. The higher input energy leads to deeper penetration and higher peak forces, but the hybrid laminate still demonstrates effective energy dissipation compared to single-fiber systems. Carbon fibers primarily carry the load at peak force due to their high modulus, while basalt fibers act as crack arrestors, bridging delaminated zones and reducing the extent of catastrophic propagation. This synergy improves the damage tolerance of the hybrid system under severe impact conditions. Comparing both velocities, it is evident that impact energy directly influences the damage mechanisms: at low velocity, deformation is absorbed mainly through matrix cracking and fiber/matrix debonding, whereas at higher velocity, fiber breakage and delamination dominate. The hybridization strategy is scientifically justified because it exploits the stiffness of carbon and the toughness of basalt, producing laminates with improved impact resistance and higher residual load-bearing capacity after impact. Literature confirms that basalt–carbon hybrids exhibit synergistic performance, outperforming pure basalt or carbon composites in terms of absorbed energy and post-impact mechanical retention.

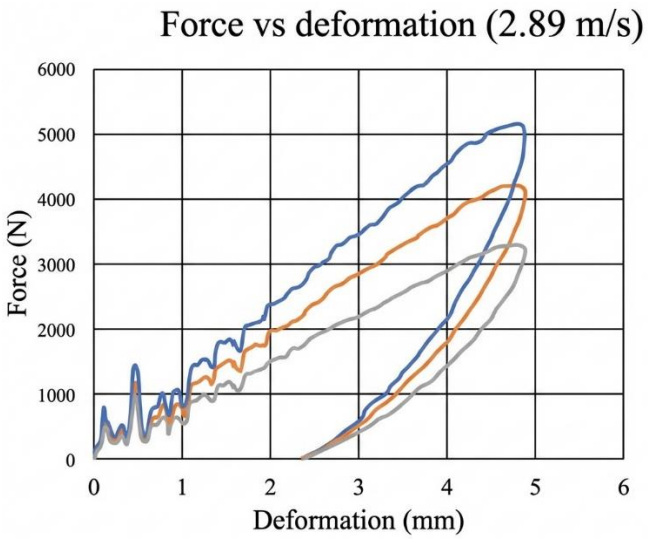

Figure 2. Force vs. deformation at 2.89 m/s.

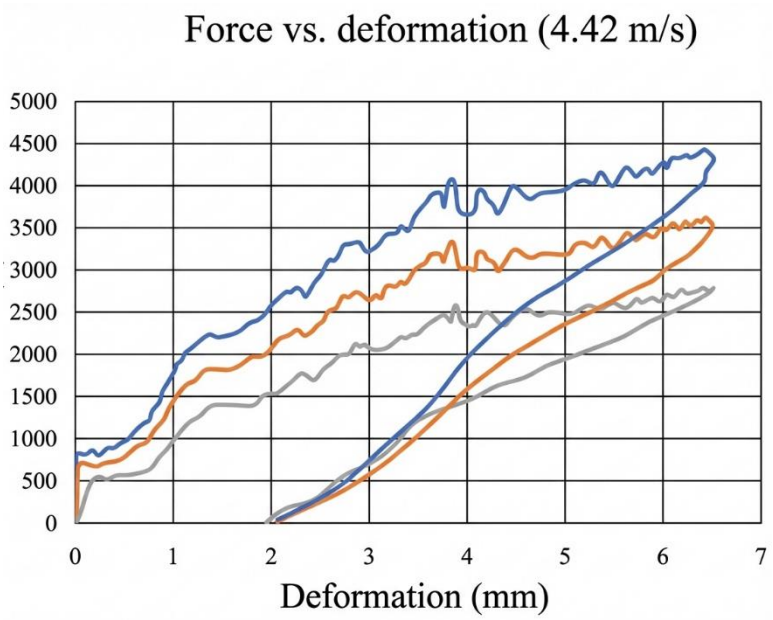

Figure 3. Force vs. deformation at 4.42 m/s.

Impact Energy vs. Deformation

At the lower speed of 2.89 m/s, the impact-energy–deformation curves Figure 4, display a steady, gradual rise in absorbed energy aligned with increasing deformation – reflecting a quasi-elastic response punctuated by matrix micro-cracking and fiber–matrix interface debonding – the optimized carbon–basalt stacking sequences significantly enhanced energy absorption under low-velocity loading by promoting controlled deformation rather than abrupt failure, the basalt fibers likely act as crack mediators, deferring catastrophic damage and sustaining energy uptake over a longer deformation path. At the higher velocity of 4.42 m/s, the curve seen in Figure 5, steepens noticeably with sharper energy uptake indicative of brittle fiber fracture and delamination onset. However, the impact does not lead to complete perforation. The carbon fibers likely bear peak loads while basalt fibers absorb fracture and delamination damage, preserving laminate integrity, by comparing it is revealed that clear the impact velocity modulates the dominant damage mode and energy absorption path.

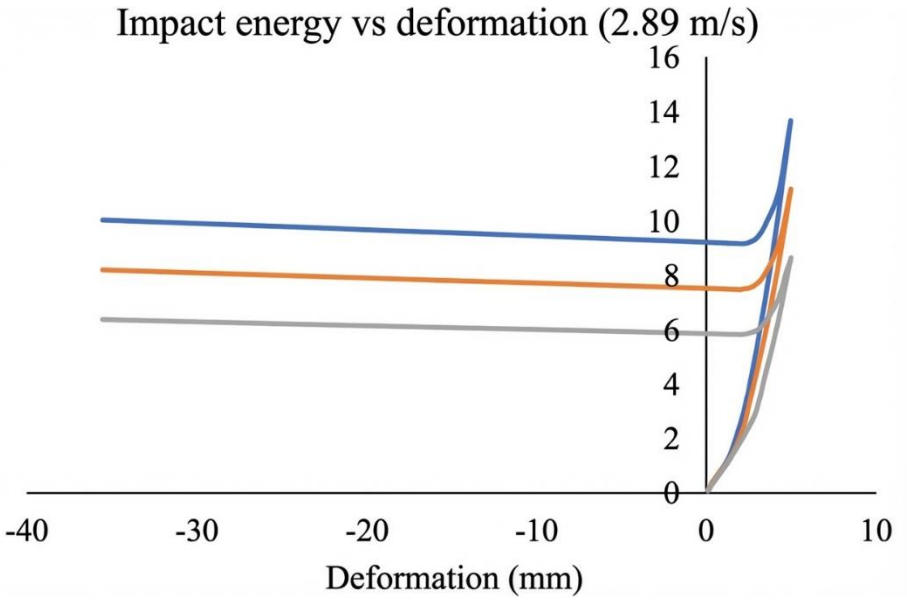

Figure 4. Impact energy vs. deformation at 2.89 m/s.

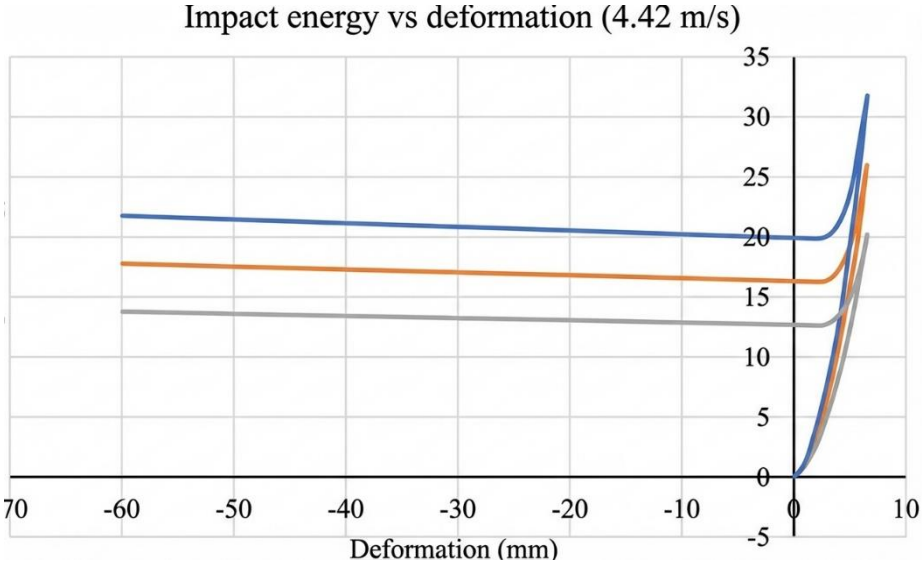

Figure 5. Impact energy vs. deformation at 4.42 m/s.

Fourier-Transform Infrared Spectroscopy

FTIR spectrum [Figure 6] of the BDM/DABPA hybrid composite shows characteristic absorption bands at 1715 cm^{-1} (C=O stretching of imide groups) and 1395 cm^{-1} (C–N stretching vibration of imide rings), confirming the successful imidization reaction during curing. Peaks around 1180–1230 cm^{-1} are attributed to C–O–C asymmetric stretching from ether linkages introduced by the DABPA allyl ether moiety. The absence or significant reduction of C=C stretching near 910–950 cm^{-1} indicates that most of the double bonds from maleimide and allyl groups have reacted during crosslinking. The broad band near 3400 cm^{-1} corresponds to O–H stretching, arising from absorbed moisture or hydroxyl groups on basalt fiber surfaces. These features collectively indicate that the hybrid network has formed a rigid aromatic BMI crosslinked structure with interfacial bonding between the resin and basalt/carbon fibers [38]. The BMPP/DABPA system, the FTIR spectrum displays in [Figure 7] strong imide carbonyl absorptions at 1710 cm^{-1} and 1775 cm^{-1}, representing asymmetric and symmetric C=O stretching vibrations. The band at 1500–1600 cm^{-1} is linked to aromatic C=C stretching of the phenyl ether segments in BMPP. Peaks near 1245 cm^{-1} correspond to Ar–O–Ar ether linkages, showing the presence of flexible phenoxy bridges from the BMPP structure. The relatively higher intensity of ether link bands compared with the BDM system suggests lower crosslink rigidity, which aligns with the lower Tg observed in DSC. Additionally, reduced absorption near 910 cm^{-1} confirms the consumption of C=C bonds during curing. The hybrid composite also shows enhanced O–H stretching around 3400 cm^{-1}, likely due to fiber–matrix interfacial interactions and hydrogen bonding with basalt hydroxyl groups [39]. Figure 8 shows the ternary BDM–BMPP–DABPA hybrid system reveals dual imide C=O bands at 1770 cm^{-1} and 1715 cm^{-1}, characteristic of highly crosslinked BMI structures. A strong absorption at 1360–1390 cm^{-1} (C–N stretching) and bands at 1180–1240 cm^{-1} (C–O–C asymmetric stretching) confirm the coexistence of BDM's rigid methylene linkages and BMPP's flexible phenoxy groups in the cured network. The broadening of the O–H band at 3400 cm^{-1} compared to the binary systems suggests improved interfacial adhesion due to synergistic hydrogen bonding and enhanced wetting of basalt fiber surfaces. The disappearance of allyl C=C absorptions (910–950 cm^{-1}) confirms full cure. Compared with Figures 1 and 2, the hybrid composite spectrum shows intensified aromatic skeletal vibrations (1600 cm^{-1}), reflecting a denser aromatic network, which correlates with the higher Tg and thermal stability [40,41]. These three FTIR analyses confirm the progressive curing reactions of BMI–DABPA systems and the role of different BMI monomers (BDM vs. BMPP) in tuning crosslink density. Carbon fibers primarily act as inert reinforcements, while basalt fibers introduce hydroxyl groups, seen as O–H stretching, that promote fiber–matrix adhesion. The ternary hybrid shows the strongest network signature (dual imide peaks with intense aromatic absorption), validating its superior thermal and mechanical stability compared to binary systems.

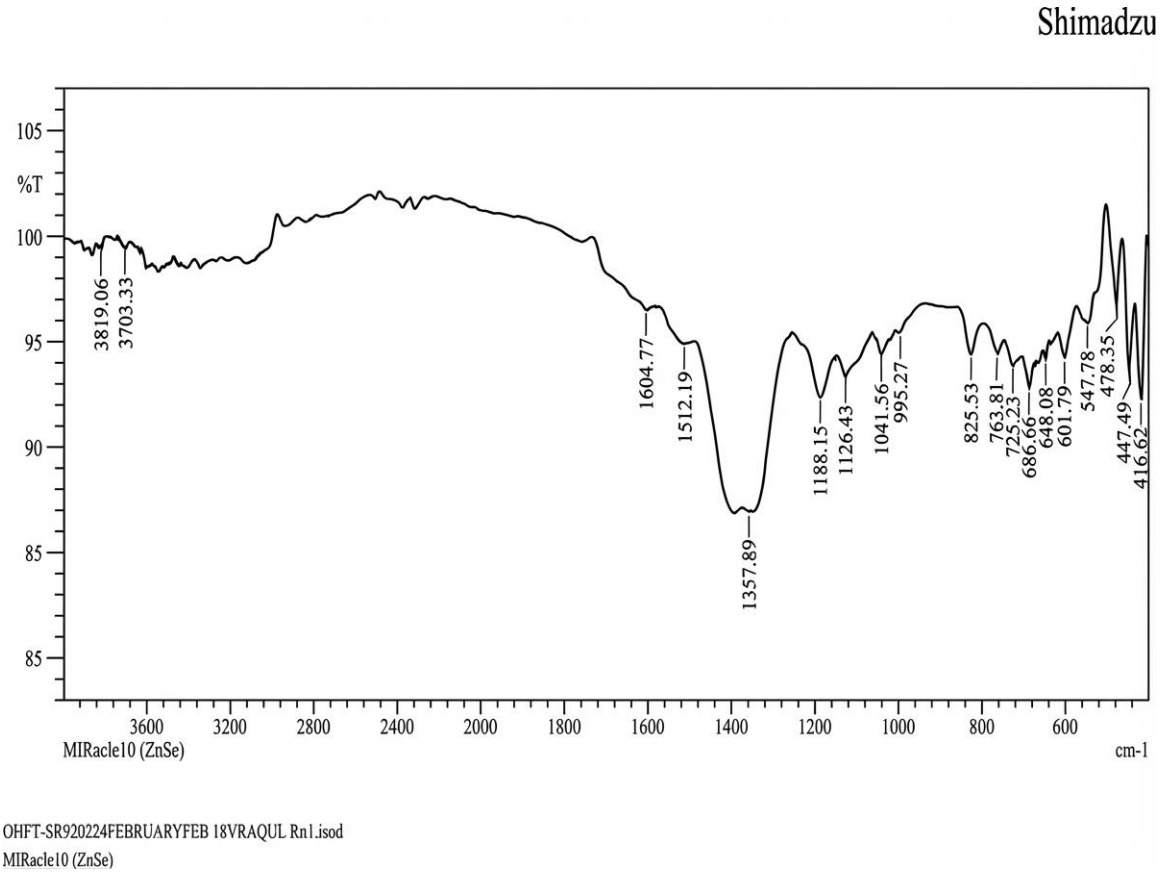

Figure 6. FTIR for sample L1.

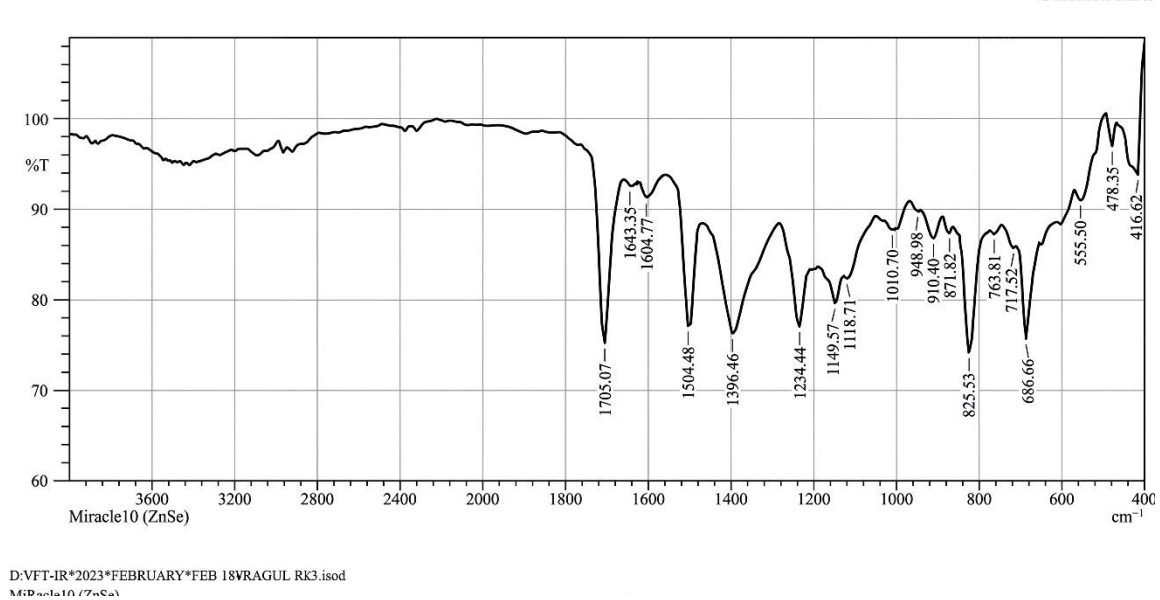

Figure 7. FTIR for sample L2.

Differential Scanning Calorimetry Studies (DSC)

The DSC trace for the BDM/DABPA laminate (Figure 8) indicates a clear baseline shift (glass transition) near 132 °C and a large endothermic/thermal event at 369–371 °C. The baseline shift is the glass transition temperature (Tg) of the cured aromatic bismaleimide network; Tg in BMI/allyl systems reflects the high crosslink density produced by maleimide–ene (Alder-ene / Michael-type) chemistry

between the maleimide (BDM) and allyl groups in DABPA. The high-temperature endotherm in this region is not a simple melting of a crystalline phase but corresponds to high-temperature thermal events associated with the decomposition/post-cure behavior of the aromatic BMI network (residual heat of reaction and eventual thermal degradation of the imide/polymeric network). This behavior (distinct cure exotherm(s) at lower temperatures followed by a high-temperature decomposition/endotherm) is well documented for 4,4′-bismaleimidodiphenylmethane (BDM)/DABPA systems and is explained by competing cure pathways (maleimide homopolymerization, ene reactions and side-reactions) that set the final crosslink architecture and Tg. In (Figure 10) the BMPP/DABPA trace displays a lower baseline Tg (115 °C) and an endothermic feature/peak in the 140–155 °C region, with decomposition onset at a noticeably lower temperature than the pure BDM system (your data shows end-set 213 °C for the observed event). This pattern is explained by the chemical structure of BMPP-type bismaleimides (bis-phenoxy-linked BMI monomers): the phenoxy linkers and larger, more flexible bridging groups in BMPP lower the processing/melting temperature and reduce the local crosslink density per unit volume compared with a BDM matrix, producing a lower observed Tg and lower-temperature thermal transitions. In DSC, the mid-range endotherm reflects either (a) melting/softening of residual low-melting monomeric fractions or (b) a cure-related thermal event (partial cure or secondary reactions). BMPP formulations are commonly used to tune the processing window and reduce melt viscosity, so a lower temperature DSC peak is expected. Figure 11 shows The hybrid BMI trace (BDM + BMPP + DABPA) shows the highest observed Tg (144 °C) and a strong endothermic/decomposition event at much higher temperature (a pronounced endotherm/peak in the 285–331 °C region and good mass retention on TGA). The increase in Tg and in the onset of high-temperature events is explained by synergistic network formation: mixing two aromatic BMI monomers (BDM and BMPP) with allyl DABPA produces a denser, more heterogeneous crosslinked network (multiple reactive groups, different local stiffness), which raises the effective crosslink density and restricts segmental mobility, hence higher Tg and improved thermal resistance. In addition, mixed-BMI systems commonly show broadened but higher-temperature cure signatures because different monomers react at slightly different temperatures and some residual curing can continue during heating, giving stronger thermostability in DSC and TGA [42,43].

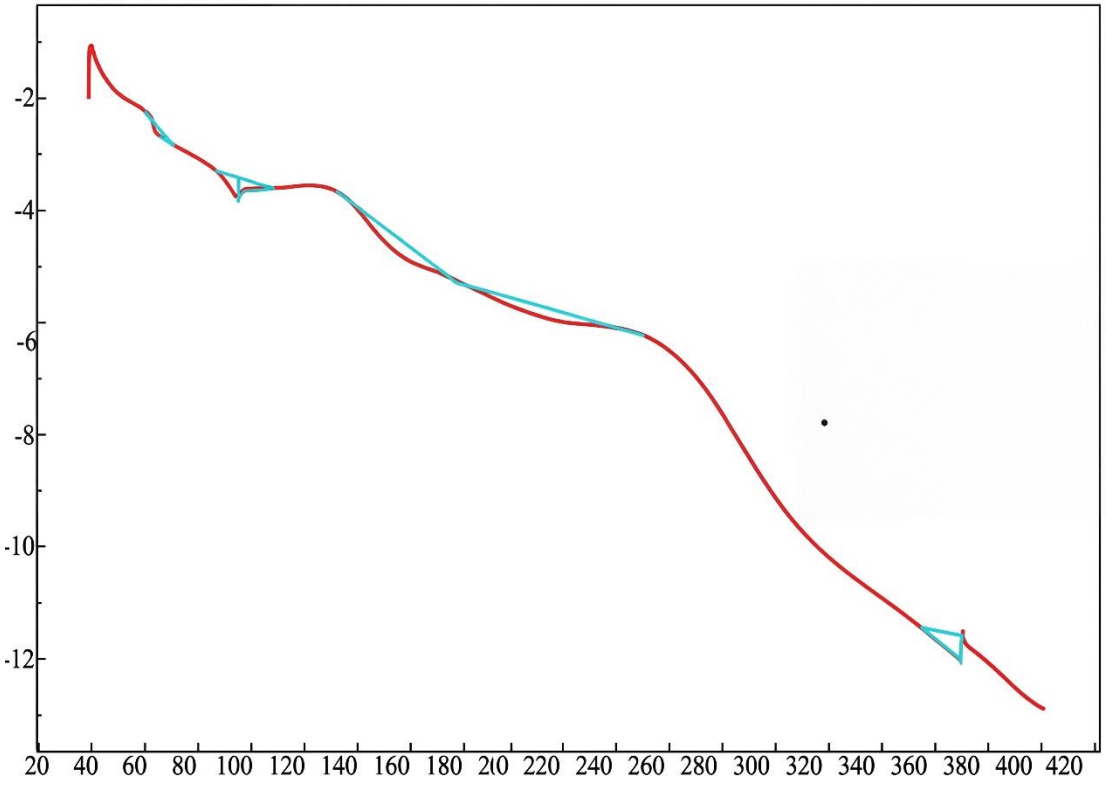

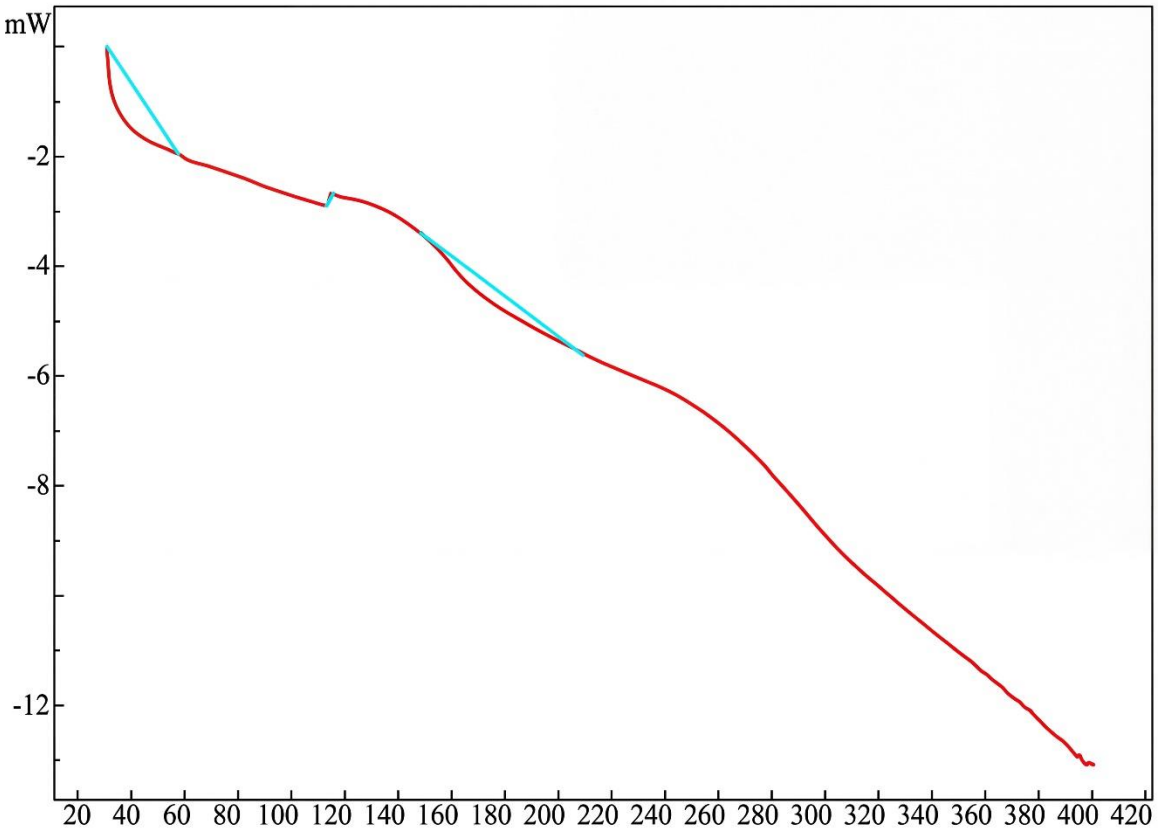

Figure 8. DSC for sample L1 and L2 (temperature vs. heat flow).

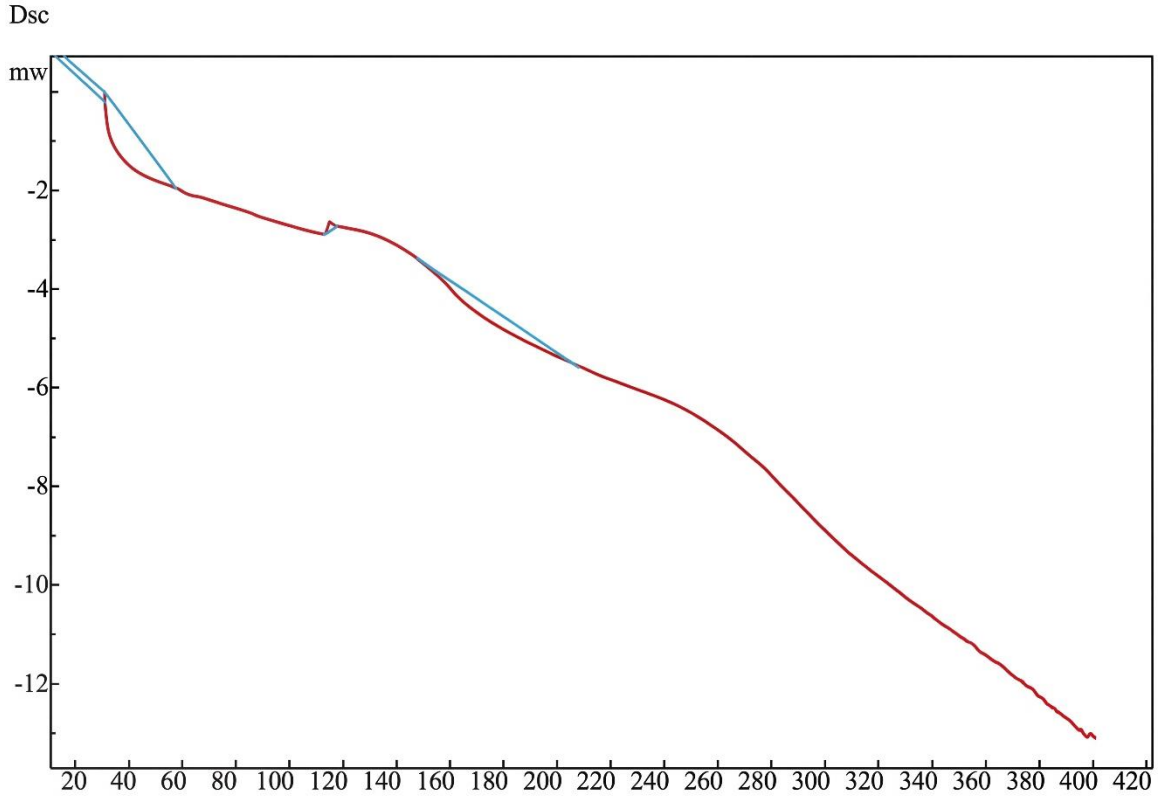

Figure 9. DSC for sample L3 (temperature vs. heat flow).

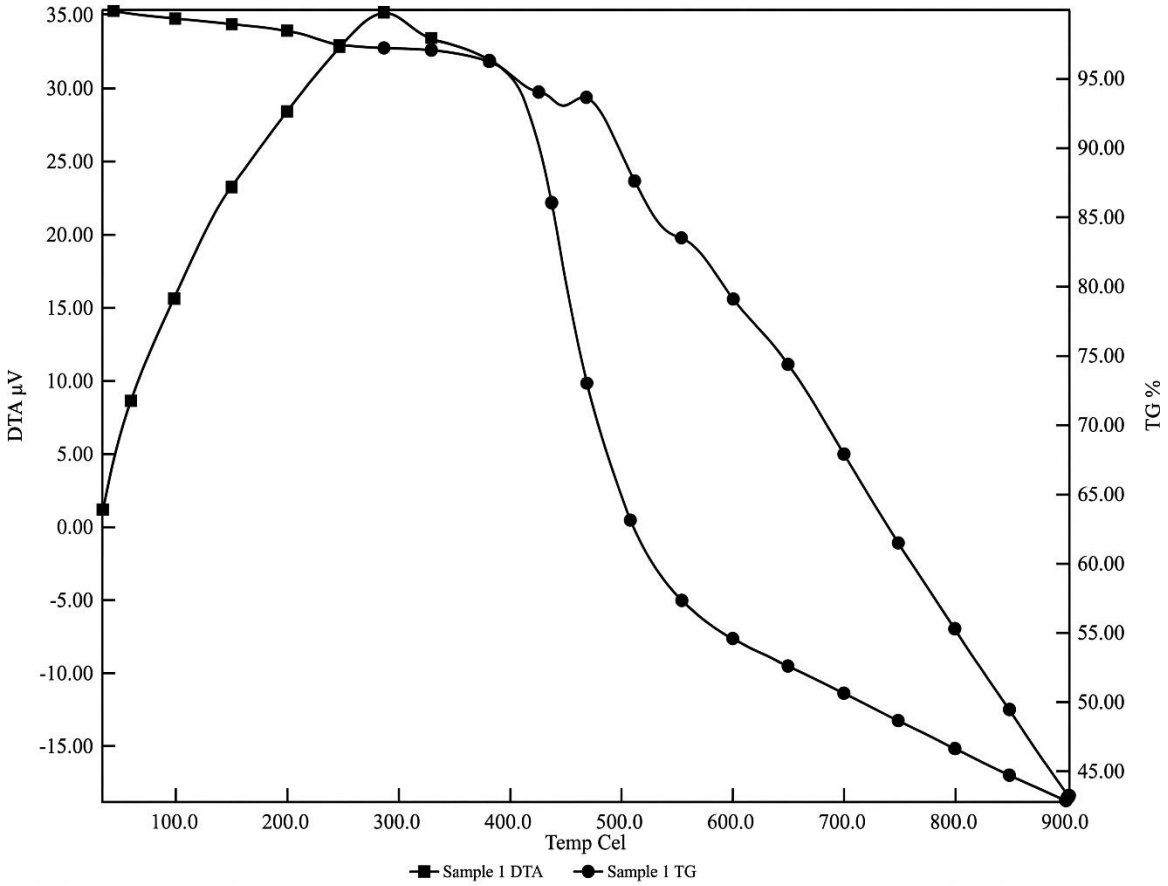

Figure 10. DTG curve for L1.

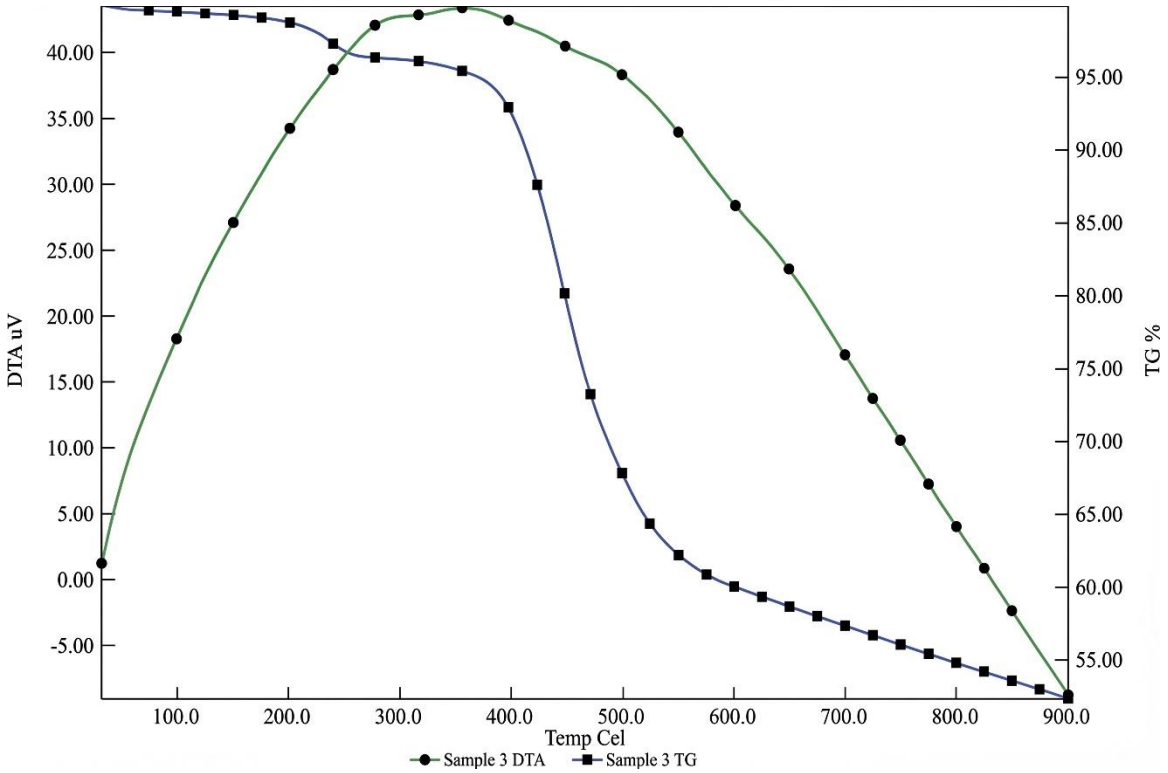

Figure 11. DTG curve for L2.

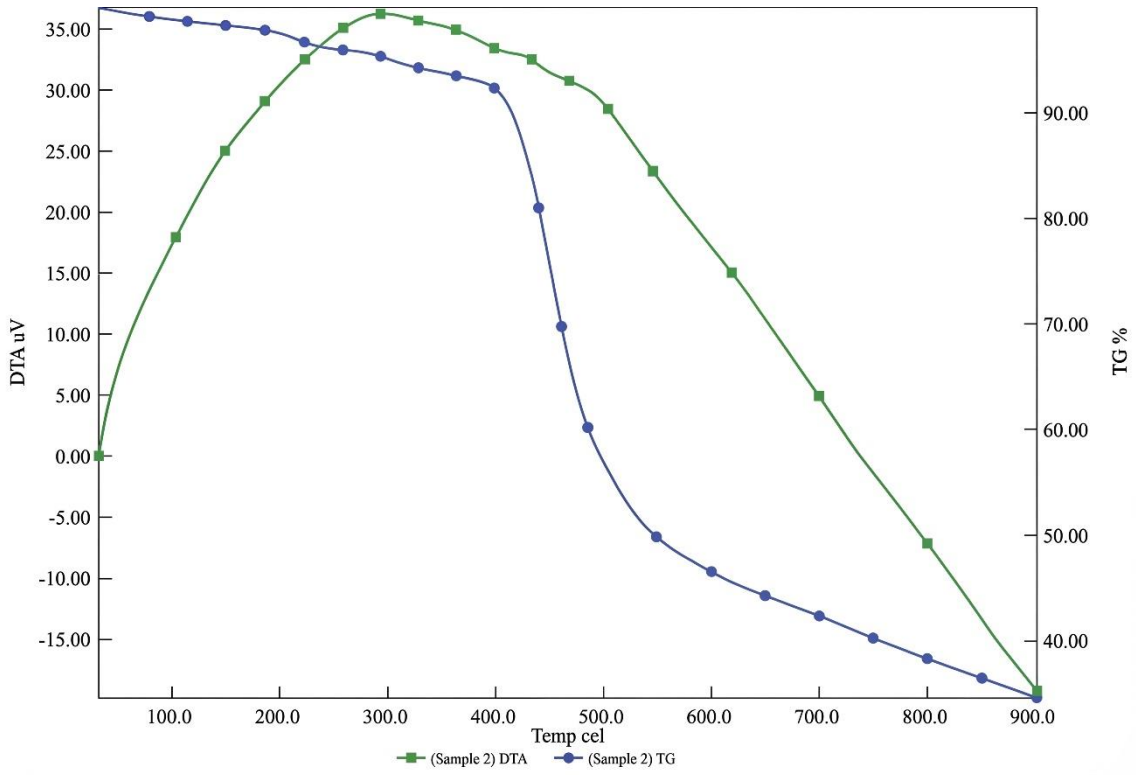

Figure 12. DTG curve for L3.

Figure 10–12 shows the DTG curve of L1–L3, L1 shows degradation onset at 280–300 °C, associated with volatilization of oligomeric residues. A major decomposition peak appears around 460 °C, corresponding to breakdown of the polyimide/phenolic backbone. The char yield of 42% at 900 °C indicates efficient carbonization, enhanced by the thermal barrier effect of basalt and carbon fibers. This thermal stability reflects the ability of phenolic domains to promote char formation, consistent with reports that hybrid basalt–carbon laminates exhibit delayed decomposition and elevated residue yield due to fiber–matrix synergy [37]. Similar findings in basalt/kevlar systems also showed stability above 350 °C, with robust char formation enhancing flame resistance. For L2, degradation commences earlier, at 200 °C, reflecting the lower stability of BMPP-derived structures. The main DTG peak near 450 °C and a char yield of 30% at 900 °C indicate reduced thermal resistance compared to L1 and L3. The sharp weight-loss profile suggests faster chain scission and less efficient char formation, highlighting the critical role of resin chemistry in degradation kinetics. The resin crosslink density governs char morphology, which results in observed similar early-onset degradation in less stable hybrid systems.

The L3 laminate exhibits the highest thermal stability, with degradation onset delayed to 400 °C and a broad, gradual decomposition event between 360–370 °C. Notably, the char retention (52% at 900 °C) is the highest among the three laminates, confirming enhanced oxidative stability and superior thermal shielding. This behavior arises from synergistic crosslinking in the resin network combined with the thermal resistance of basalt and carbon fibers. Similar results are reported that optimized resin fiber hybridization improves char yield and slows volatile release, also the role of basalt in stabilizing char structure and enhancing flame resistance in hybrid laminates.

CONCLUSIONS

In this study, high-performance polyimide/phenolic resin systems (BDM/DABPA, BMPP/DABPA, and BDM/BMPP/DABPA) were used to successfully fabricate and characterize hybrid basalt–carbon fiber laminates. Improved fiber–matrix adhesion, decreased porosity, and increased structural integrity were the results of the hybrid processing method and multi-step curing. Low-velocity impact tests

showed that hybridization successfully balanced toughness and stiffness, with carbon fibers maintaining load-bearing capacity and basalt fibers preventing catastrophic fracture through crack bridging. Of the systems that were tested, the BDM/BMPP/DABPA hybrid showed the highest impact energy absorption (14 J at 2.89 m/s and 32 J at 4.42 m/s), the highest char yield (52% at 900 °C), and superior thermal stability with onset of degradation above 400 °C. It is confirmed that higher glass-transition temperature and stronger crosslink density in the ternary system, while DTG results validated its superior oxidative resistance compared to binary systems.

REFERENCES

1. Cantwell WJ, Morton J. *The impact resistance of composite materials—A review.* Composites. 22(5):347–362. https://doi.org/10.1016/0010-4361(91)90549-V,1991
2. Abrate S. *Impact on laminated composite materials*. Appl Mech Rev. 1991;44(4):155–190. https://doi.org/10.1115/1.3119500
3. Richardson MOW, Wisheart MJ. *Review of low-velocity impact properties of composite materials*. Compos Part A. 1996;27(12):1123–1131. https://doi.org/10.1016/1359-835X(96)00074-7
4. Zhang X, Hounslow L, Grassi M. *Improved low-velocity impact modelling of composite laminates.* Compos Sci Technol. ;69(7–8):805–812. 2009. https://doi.org/10.1016/j.compscitech.2009.01.019
5. Reis P, Fangueiro R, Pereira A. *Mitigation strategies in laminate low-velocity impact*. Polym Compos. 2024;45(10):1874–1888. https://doi.org/10.1002/pc.27675.
6. Safri SNA, Sultan MTH, Jawaid M, Jayakrishna K. *Impact behaviour of hybrid composites for structural applications: A review.* Compos Part B. 2018;133:112–121. https://doi.org/10.1016/j.compositesb.2017.09.008
7. Sarasini F, Tirillò J, Valente T, *Drop-weight impact behaviour of woven hybrid basalt–carbon/epoxy composites.* Compos Part B. 2014;59:204–220. https://doi.org/10.1016/j.compositesb.2013.12.006
8. Tirillò J, Sarasini F, Lampani L, et al. High-velocity impact behaviour of hybrid basalt–carbon/epoxy composites. Compos Struct. 2017;168:305–312. https://doi.org/10.1016/j.compstruct.2017.02.039
9. Fiore V, Scalici T, Di Bella G, Valenza A. *A review on basalt fibre and its composites.* Compos Part B. 2015;74:74–94. (2014) https://doi.org/10.1016/j.compositesb.2014.12.034
10. Kessler E, Gadow R, Straub J. *Basalt, glass and carbon fibers and their composites under thermal and mechanical load.* AIMS Mater Sci. ;3(4):1561–1576. doi.org/10.3934/matersci.2016.4.15612016
11. Pu, Y., Liu, B., Xue, G., Liang, H., Ma, F., Yang, M., & Tian, G. *Carbon/Basalt Fibers Hybrid Composites: Hybrid Design and the Application in Automobile Engine Hood*. Polymers, 14(18),3917. doi.org/10.3390/polym14183917,(2022).
12. Gür M, Yildizhan M, Avci A. *Ballistic and flexural resistance of basalt–carbon/glass hybrid composites.* Polym Compos. 2024;45(2):337–348. https://doi.org/10.1002/pc.27569
13. Duan, S.-J., Feng, R.-M., Yuan, X.-Y., Song, L.-T., Tong, G.-S., & Tong, J.-Z. (2025). *A Review on Research Advances and Applications of Basalt Fiber-Reinforced Polymer in the Construction Industry.* Buildings, 15(2), 181. https://doi.org/10.3390/buildings15020181.
14. Liu Y, *Polyimide ablative/thermal insulation composites: A review.* J Thermoplast Compos Mater. 2022;35(12):1690–1714. https://doi.org/10.1177/08927057211050665
15. Ma J, Liu X, Wang R, *Research progress and application of polyimide-based nanocomposites.* Nanomaterials. 2023;13(4):656. https://doi.org/10.3390/nano13040656
16. Chen W-C, Liu Y-T, Kuo S-W. DDSQ-modified phenolic resins with enhanced thermal stability. Polymers. 2020;12(10):2238. https://doi.org/10.3390/polym12102238
17. Zhang Y, et al. Thermal-protective coatings on PI-based glass-fiber composites. Polym Compos. 2024;45(3):915–927. https://doi.org/10.1002/pc.27894
18. Liu Y, et al. Review of FRP phenolic thermal-protection materials. Energies. 2025;18(4):819. https://doi.org/10.3390/en18040819

19. Kumar CV, Kandasubramanian B. *Advances in ablative composites of carbon-based materials*: A review. Ind Eng Chem Res. 2019;58(51):22663–22701. https://doi.org/10.1021/acs.iecr.9b04625
20. Zhu, Y., Zhang, J., Wang, L., & Guo, Q. (2025*). Ballistic impact response of hybrid carbon/basalt fiber-metal laminates*. Composites Part B: Engineering, 295, 111123. https://doi.org/10.1016/j.compositesb.2025.111123
21. Zhang, H., Li, Y., & Xu, Z. (2025). *Low-velocity impact behavior of hybrid basalt/carbon FRP laminates.* Case Studies in Construction Materials, 23, e02345. https://doi.org/10.1016/j.cscm.2025.e02345
22. Khan, M. A., Ali, S., & Rehman, Z. U. (2025). *Damage mechanisms of basalt/carbon fiber hybrids under impact loading.* Polymers, 17(7), 866. https://doi.org/10.3390/polym17070866
23. Liu, J., Wang, X., & Zhao, Y. (2022). *Polyimide-based ablative and thermal insulation composites: A review*. Journal of Thermoplastic Composite Materials, 35(10), 1403–1426. https://doi.org/10.1177/08927057211025630
24. Xiong, X., Zhang, W., Li, H., Wang, D., & Chen, Z. (2024). *Cure kinetics and thermal degradation behavior of polyimide resin systems studied by TGA and kinetic modeling*. Polymers, 16(8), 1149. https://doi.org/10.3390/polym16081149
25. Kok, R., Rao, V., Sain, M., Deb, S., Mallick, P., Lekberg, N., & Cockcroft, H. (2024). *Low-velocity impact response of automated fiber placement composites: influence of internal architecture*. Composites Part B: Engineering, 271, 111154. https://doi.org/10.1016/j.compositesb.2024.111154
26. Rajak, D. K., Shrivastava, A., & Srivastava, R. (2020). *Influence of cutting process on the mechanical and thermal performance of fiber-reinforced composites.* Journal of Materials Processing Technology, 283, 116706. https://doi.org/10.1016/j.jmatprotec.2020.116706
27. Fiore, V., Scalici, T., Di Bella, G., & Valenza, A. *A review on basalt fibre and its composites.* Composites Part B: Engineering, 74, 74–94. (2015). https://doi.org/10.1016/j.compositesb.2014.12.034.
28. Pramoda, K. P., Bhowmick, A. K., & Okamoto, M. *Characterization and thermal degradation of polyimide and related aromatic polymers*. Polymer Degradation and Stability, 70(1), 35–44. https://doi.org/10.1016/S0141-3910(00)00138-X,(2000).
29. Alshehri, A. H., Johari, M. A. M., & Aravinthan, T. (2024). *Investigating low velocity impact and compression-after-impact behaviors of carbon fiber composites.* Polymer Composites, 45(6), 1234–1245. https://doi.org/10.1002/pc.30112
30. Sarasini, F.; Tirillò, J.; D'Altilia, S.; Valente, T.; Cioffi, S.; Iannace, S.; Sorrentino, L. *Hybrid composites based on basalt and carbon fibers: Impact damage and residual flexural properties*. Composites Part B: Engineering, 2016, 111, 76–89. DOI: 10.1016/j.compositesb.2016.12.011.
31. Karuppiah G, Kuttalam KC, Palaniappan M, Santulli C, Palanisamy S. Multiobjective Optimization of Fabrication Parameters of Jute Fiber/Polyester Composites with Egg Shell Powder and Nanoclay Filler. Molecules. 2020; 25(23):5579. https://doi.org/10.3390/molecules25235579.
32. . Padmanabhan R.G , S. Rajesh,S. Karthikeyan, Sivasubramanian Palanisamy, . Ilyas R.A, Nadir Ayrilmis , ElSayed M. Tag-eldin, Mohamed Kchaou ,Evaluation of mechanical properties and Fick's diffusion behaviour of aluminum-DMEM reinforced with hemp/bamboo/basalt woven fiber metal laminates (WFML) under different stacking sequences, Ain Shams Engineering vol.15,7,pp102759, 2024 ,https://doi.org/10.1016/j.asej.2024.102759.
33. Ayrilmis N, Kanat G, Yildiz Avsar E, Palanisamy S, Ashori A. Utilizing waste manhole covers and fibreboard as reinforcing fillers for thermoplastic composites. *Journal of Reinforced Plastics and Composites*. 2024;44(17-18):1108-1118. https://doi:10.1177/07316844241238507
34. Rajkumar Ramasubbu, Arumugam Kayambu, Sivasubramanian Palanisamy, and Nadir Ayrilmis Mechanical Properties of Epoxy Composites Reinforced with Areca catechu Fibers Containing Silicon Carbide , Bioresources, 19 (2), 2353–2370, https:// doi: 10.15376/biores.19.2.2353-2370.
35. Aruchamy, K., Karuppusamy, M., Krishnakumar , S., Palanisamy, S., Jayamani, M., Sureshkumar , K., Ali, S. K., and Al-Farraj, S. A. Enhancement of mechanical properties of hybrid polymer composites using palmyra palm and coconut sheath fibers: The role of tamarind shell powder,(2025). Bio-Resources 20(1), 698–724. https:// doi: 10.15376/biores.20.1.698-724.

36. Arup Kar, Dip Saikia, Sivasubramanian Palanisamy, Narayanasamy Pandiarajan, Effect of fiber loading on the mechanical, morphological, and dynamic mechanical characteristics of Calamus tenuis fiber reinforced epoxy composites, Volume 31, Issue 1, Pages 224-2402025,. https:// doi: 10.1002/vnl.22167.
37. Morgan, R. J., Shin, E., & Jurek, R. J. (1997). *Characterization of the cure reactions of bismaleimide composite matrices.* Polymer, 38(3), 639–646. https://doi.org/10.1016/S0032-3861(96)00542-3
38. Guo, Q.-W., Zhang, G.-L., & Li, J.-L. (2014). *Kinetic study of a bismaleimide resin curing process by differential scanning calorimetry and rheological analysis*. Journal of Reinforced Plastics and Composites. https://doi.org/10.1177/0731684414544390
39. Phelan, J. C., & Sung, C. S. P. *Cure characterization in bis(maleimide)/diallylbisphenol A resin by fluorescence, FT-IR, and UV-reflection spectroscopy.* Macromolecules, 30(22), 6845–6851.(1997). https://doi.org/10.1021/ma961887f.
40. Vijayakumar, C. T.; Surender, R.; Rajendran, K.; Alam, S. *Synthesis and thermal studies of bisphenol-A based bismaleimide.* Journal of Thermal Analysis and Calorimetry 2011, 103, 693–699. DOI: 10.1007/s10973-010-1020-5.(2011)
41. Wolter, N.; Beber, V. C.; Sandinge, A.; Blomqvist, P.; Goethals, F.; Van Hove, M.; Jubete, E.; Mayer, B.; Koschek, K. *Carbon, Glass and Basalt Fiber Reinforced Polybenzoxazine: The Effects of Fiber Reinforcement on Mechanical, Fire, Smoke and Toxicity Properties*. Polymers (Basel) 2020, 12(10), 2379. DOI: 10.3390/polym12102379.
42. Sabzi, S. S., Karimzadeh, F., & Ardjmand, M. *Thermal degradation behavior and kinetics of basalt/carbon fiber hybrid composites using TGA–DTG analysis.* Journal of Thermal Analysis and Calorimetry, 145(5), 3053–3065. (2024). https://doi.org/10.1007/s10973-023-11805-2
43. Singh, R., Patel, N., & Kumar, A. *Thermal stability and flame-retardant properties of a basalt/kevlar fiber-reinforced hybrid polymer composite with bran filler particulates*. Results in Engineering, 22, 104207. (2025). https://doi.org/10.1016/j.rineng.2025.104207.

